Intramolecular Electronic Energy Transfer between Naphthalene and Protoporphyrin Chromophores Bound to Sequential Peptides

Basilio Pispisa,*,† Mariano Venanzi,† Antonio Palleschi,‡ and Giancarlo Zanotti§

Dipartimento di Scienze e Tecnologie Chimiche, Università di Roma "Tor Vergata", 00133 Roma, Italy, Dipartimento di Chimica, Università di Roma "La Sapienza", 00185 Roma, Italy, and Centro di Chimica del Farmaco, c/o Dipartimento di Studi Farmaceutici, Università di Roma "La Sapienza", 00185 Roma, Italy

Received May 19, 1994; Revised Manuscript Received September 20, 1994®

ABSTRACT: The photophysics of a series of peptides carrying naphthalene and protoporphyrin IX, covalently bound to ϵ-amino groups of lysine residues were investigated in methanol solution by steady-state and time-resolved fluorescence experiments, as well as by transient absorption spectra. The general formula of the series is Boc-Leu-Leu-Lys-$(Ala)_n$-Leu-Leu-Lys-OtBu, where Leu = L-leucine, Lys = L-lysine, Ala = L-alanine, and $n = 0-4$. Quenching of excited naphthalene takes place by electronic energy transfer and proceeds on a time scale of 3−8 ns. A minor and slower (≈45 ns) fluorescence decay was also measured, which was ascribed to exciplex quenching since it does not depend on the interchromophoric distances. IR spectra in methanol solution indicate that intramolecularly H-bonded conformations form, and circular dichroism data in both methanol and water−methanol mixtures suggest the presence of variable amounts of α-helix structure, depending on the chain length. The probability distribution of center-to-center distances of chain-linked donor-acceptor pairs was calculated by a rotational isomeric states model, in which rotation around each bond in the chromophore linkages is restricted to a few highly populated, low-energy isomeric states. By using the calculated distributions and applying a Förster type mechanism, the kinetics of the energy transfer were satisfactorily reproduced for all the compounds investigated only when the mutual orientations of the chromophores were also taken into account because interconversion among conformational substates of probe linkages is slow on the time scale of the transfer process.

Introduction

We have recently studied the influence of conformational equilibria of poly(L-lysine) (PL) in aqueous solution on the photophysics of protoporphyrin IX (P) and 1-naphthylacetic acid (N) covalently bound to ϵ-amino groups of the side chains.[1] On going from the disordered (pH 7) to the ordered polymeric matrix (pH 11), quenching of excited naphthyl chromophore in PNPL occurs by two competitive processes. One is the interconversion to the triplet state, taking place when the sample is randomly coiled, and the other is the intramolecular electron transfer from ground-state porphyrin, when the polypeptide is in α-helical conformation. Furthermore, although the chromophores were bound to the main chain by a rather long spacer, both polarized fluorescence and differential circular dichroism (DCD) spectra clearly indicated that they experience a rotational mobility definitely more hindered than the polymer-free molecules. This was chiefly ascribed to the amide bond in the substituted side chains, the effect being enhanced by the α-helical conformation of the backbone chain that makes the whole structure more stiff.[1b]

α-Helical polypeptides represent good molecular carriers for spatially fixed chromophores,[2] but sequential oligopeptides provide a better means for studying the dependence of the rate of intramolecular excited-state processes on the separation distance of the fluorophores, as well as on the chemical and structural features of the intervening amino acids.[3-5]

Chart 1

Boc- Leu-Leu-Lys-$(Ala)_n$-Leu-Leu-Lys-*OtBu*

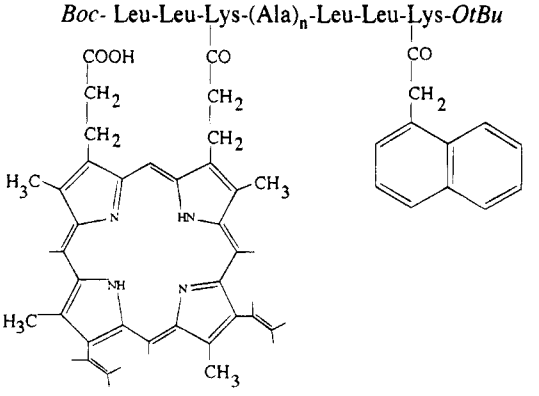

We then studied the photophysics in methanol solution of a series of sequential peptides carrying the same molecules as those mentioned above, i.e., protoporphyrin IX and 1-naphthylacetic acid covalently bound to the ϵ-amino group of lysine residues. This series is formed by two Leu-Leu-Lys triads (Leu = L-leucine; Lys = L-lysine) linked together through a spacer of $n = 0-4$ L-alanine (Ala) residues, as represented in Chart 1. Owing to the presence of two carboxylic groups in P, both monomeric and cross-linked dimeric protoporphyryl peptides were synthesized, but only the monomeric species will be reported here. They will be denoted as $P(Ala)_nN$ ($n = 0-4$) and the corresponding blank samples as $(Ala)_nN$ and $(Ala)_nP$, depending on the bound chromophore.

The separation distance between P and N groups is expected to increase with the number of alanyl groups. However, where the backbone chain attains an ordered, intramolecularly H-bonded structure, which should be

† Università di Roma "Tor Vergata".
‡ Dipartimento di Chimica, Università di Roma "La Sapienza".
§ Centro di Chimica del Farmaco, Università di Roma "La Sapienza".
® Abstract published in *Advance ACS Abstracts,* November 1, 1994.

0024-9297/94/2227-7800$04.50/0 © 1994 American Chemical Society

favored by the good α-helix-forming Leu and Ala residues,[6,7] a periodic variation in the interchromophoric distances is predictable. This is indeed the case, but, unexpectedly, quenching of naphthalene fluorescence does not take place by electron transfer from protoporphyrin, as observed in the α-helical PNPL,[1] but by intramolecular electronic energy transfer. Therefore, the $e^{-\beta R}$ dependence of the electron transfer rate[1b,3b] appears to be better accomplished in a rigid environment, such as the long helical chain of the polypeptide, than in a flexible frame, such as the short α-helical segment of the oligopeptides, where the R^{-6}-dependent energy transfer rate[9] is apparently favored.

A preliminary account of this study was already reported,[8] but we now present new results on the excited-state behavior of the chromophores and a thorough analysis of the data by a long range dipole–dipole interaction model.[9] By combining the conformational statistics of the peptides with geometric considerations,[10-12] we were able to evaluate the distribution probability of the center-to-center distances between N and P molecules, arising from the conformational mobility of the aliphatic portion of the chromophores linkages, and reproduce the kinetics of the excited-state process.

Experimental Section

Materials. Identity and purity of all peptides were checked by amino acid, ^1H NMR, high-resolution mass spectrometry (FAB), and thin-layer chromatography analyses, using silica gel Merck plates.

The following abbreviations are used throughout: Boc, *tert*-butyloxycarbonyl; Z, benzyloxycarbonyl; Ddz, α,α-dimethyl-[(3,5-dimethoxybenzyl)oxy]carbonyl; OMe, methyl ester; OtBu, *tert*-butyl ester; OBg, *N*-(benzylhydryl)glycolamide ester; Ac, acetyl; iBCCl, (isobutyloxy)carbonyl chloride; NAc, naphthylacetyl (in Chart 1 simply denoted as N); NMM, *N*-methylmorpholine; DMF, dimethylformamide; TFA, trifluoroacetic acid; and THF, tetrahydrofuran.

Ddz and Boc groups were used to protect the amino terminus. OMe, OtBu, and OBg were used to protect the carbonyl terminus. The removal of Ddz and Boc groups was accomplished by 3% TFA in CH_2Cl_2 and absolute TFA, respectively, while that of the OMe and OBg esters was by NaOH in H_2O/methanol and K_2CO_3 in H_2O/DMF, respectively. The Z group was used to protect the ε-amino group of Lys and removed with H_2 over a Pd/C catalyst.

The synthesis of the oligopeptides was performed by the conventional mixed anhydride (MA) method. Amino acid precursors were purchased from NOVA Biochem or Fluka, and naphthylacetic acid and protoporphyrin IX were from Aldrich. Analytical grade reagents and solvents were always used.

Boc-Leu-Leu-Lys(Z)-OH. Boc-Leu-OH (2.31 g, 10 mmol) in 50 mL of CH_2Cl_2 was treated under stirring at −10 °C with iBBCl (1.36 g, 10 mmol) and NMM (1.42 g, 14 mmol). After 10 min, H-Leu-OMe (1.45 g, 10 mmol) in 20 mL of CH_2Cl_2 was added to the MA solution. After stirring at room temperature for 3 h, the reaction mixture was washed with saturated aqueous $NaHCO_3$, 0.5 M $KHSO_4$, and water, dried over Na_2SO_4, and evaporated in vacuo to give 3.5 g (100% yield) of TLC pure Boc-Leu-Leu-OMe. R_f (diethyl ether/hexane, 75/25) = 0.8. Removal of the OMe group afforded 3 g of Boc-Leu-Leu-OH (8.7 mmol) which was reacted with H-Lys(Z)-OMe (2.55 g, 8.7 mmol) by using the MA method as described above. The compound was purified by chromatography on a silica gel column in diethyl ether/hexane (96/4) as eluant to give 2.74 g (4.4 mmol, 50% yield) of TLC pure Boc-Leu-Leu-Lys(Z)-OMe. R_f (diethyl ether/hexane, 95/5) = 0.6. The removal of OMe by saponification afforded 2.66 g of the title compound (100% yield).

Ddz-Leu-Leu-Lys-OtBu. Ddz-Leu-OH (3.53 g, 10 mmol) and H-Leu-OMe (1.45 g, 10 mmol) were coupled by the MA method, as described above, to afford 4.46 g (93% yield) of TLC pure Ddz-Leu-Leu-OMe. R_f (diethyl ether/hexane, 95/5) = 0.8. Removal of the OMe group by saponification afforded 3.95 g (8.48 mmol, 90% yield) and Ddz-Leu-Leu-OH, which was further reacted by MA with H-Lys(Z)-OtBu (2.84 g, 8.48 mmol); 4.2 g (63% yield) of TLC pure Ddz-Leu-Leu-Lys(Z)-OtBu was then obtained. R_f (diethyl ether/hexane, 75/25) = 0.4. The tripeptide in methanolic solution was eventually hydrogenated over 200 mg of 10% Pd on charcoal for 1 h at room temperature, obtaining 2.54 g (74% yield) of the title compound.

Ddz-Leu-Leu-Lys(NAc)-OtBu. Naphthylacetic acid (477 mg, 2.56 mmol) in 30 mL of CH_2Cl_2 was reacted by the MA method with 1.67 g of Ddz-Leu-Leu-Lys-OtBu (2.56 mmol). After workup as described above, 2.0 g (95% yield) of the TLC pure title compound were obtained. R_f (diethyl ether) = 0.35.

Ddz-Leu-Leu-Lys(Ac)-OtBu. Ddz-Leu-Leu-Lys-OtBu (1.02 g, 1.57 mmol) dissolved in 10 mL of THF was treated with 0.2 mL of NMM and 147 mg (1.88 mmol) of acetyl chloride. After the mixture was stirred for 1 h at room temperature, the solvent was evaporated in vacuo and the residue, taken up in $CHCl_3$, was washed with saturated aqueous $NHCO_3$, 0.5 M $KHSO_4$, and water, dried over Na_2SO_4, and evaporated to give 1.08 g (100% yield) of the TLC pure title compound. R_f ($CHCl_3$/CH_3OH, 95/5) = 0.8.

Boc-Leu-Leu-Lys(Z)-(Ala)$_n$-OBg. General procedure: the sequential Boc-(Ala)$_n$-OBg peptides were synthesized by stepwise MA coupling of Boc-Ala-OH with H-(Ala)$_n$-OBg. The Boc group was cleaved from the Boc-(Ala)$_n$-OBg peptides by absolute TFA; 1.2 g of Boc-Leu-Leu-Lys(Z)-OH (2 mmol) was coupled by MA with 2 mmol of H-(Ala)$_n$-OBg. The reaction residue was purified by chromatography on silica gel columns in $CHCl_3$/CH_3OH (9/1) as eluant. R_f ($CHCl_3$/CH_3OH, 9/1) = 0.55 (*n*1), 0.60 (2), 0.55 (3), and 0.50 (4); yields: 85, 90, 57, and 65%, respectively. The OBg ester was cleaved by treating 2 mmol of each peptide in 20 mL of DMF with 555 mg of K_2CO_3 (4 mmol) in 10 mL of water for 2 h at room temperature. The reaction mixture, washed with diethyl ether and acidified to pH 3 with $KHSO_4$, was extracted several times with ethyl acetate. The collected organic phases, washed with water and dried over Na_2SO_4, were evaporated in vacuo to afford the pure Boc-Leu-Leu-Lys(Z)-(Ala)$_n$-OH compounds (see below).

Boc-Leu-Leu-Lys-(Ala)$_n$-Leu-Leu-Lys(NAc)-OtBu. General procedure: 1 mmol of Boc-Leu-Leu-Lys(Z)-(Ala)$_n$-OH in 30 mL of CH_2Cl_2–DMF (1:1 was treated at −10 °C with 136 mg of iBCCl (1 mmol) and 136 mg of NMM (1.34 mmol) under stirring. After 10 min, the solution of the amino component, prepared as follows, was added to this solution. Ddz-Leu-Leu-Lys(NAc)-OtBu (818 mg, 1 mmol) in 30 mL of CH_2Cl_2 was treated with 0.76 mL of TFA (10 mmol) for 30 min at room temperature to cleave the Ddz group and then neutralized by 1.1 mL of NMM (10 mmol). After 3 h of stirring at room temperature, the reaction mixture was washed with saturated aqueous $NaHCO_3$ solution, 0.5 M $KHSO_4$, and water, dried over Na_2SO_4, and evaporated to give a residue that was chromatographed on a Sephadex LH 20 column (2.5 × 250 cm) in CH_3OH as eluant to afford the pure title compounds. R_f ($CHCl_3$/CH_3OH, 95/5) = 0.30 (*n* = 0), 0.30 (1), 0.30 (2), 0.35 (3), and 0.25 (4); yields: 60, 36, 50, 50, and 15%, respectively. The Z group was removed by hydrogenolysis in methanol solution over 10% Pd on activated carbon for 24 h at room temperature.

Boc-Leu-Leu-Lys-(Ala)$_2$-Leu-Leu-Lys(Ac)-OtBU. The title compound was prepared as a blank sample. It was obtained from Boc-Leu-Leu-Lys(Z)-(Ala)$_2$-OH and Ddz-Leu-Leu-Lys(Ac)-OtBu following the same procedure described above. R_f ($CHCl_3$/CH_3OH, 95/5) = 0.30; yield: 30%.

Protoporphyryl Peptides. General procedure: 281 mg of protoporphyrin IX (0.5 mmol) was dissolved in 5 mL of DMF and treated at −10 °C with 78 mg of iBCCl (0.5 mmol) and 101 mg of NMM (1 mmol). After 10 min, a precooled solution of 0.5 mmol of the above-described amino peptide component was added. The reaction mixture was stirred at room temperature for 4 h and then evaporated in vacuo. The residue, treated with 10 mL of CH_3OH, was filtered from the unsoluble material and the filtrate evaporated and chromatographed on a Sephadex LH 20 column (2.5 × 250 cm) using methanol as eluant. The fractions containing the protoporphyryl peptides were collected and evaporated, and the residue was further

chromatographed on a silica gel column (2 × 50 cm) in $CHCl_3$/CH_3OH (9/1) as eluant, in order to separate the monomeric from the dimeric peptides. Monomeric compounds: R_f($CHCl_3$/CH_3OH, 9/1) = 0.20 (n = 0), 0.25 (1), 0.30 (2), 0.30 (3), and 0.30 (4); yields = 8.5, 8, 8, 3, and 4.5%, respectively, those of the blank (having acetyl instead of naphthylacetyl; see above) being 0.40 and 10%. FAB (trinitrobenzyl alcohol matrix): *m/e* calcd for $C_{91}H_{126}O_{13}N_{12}$, $C_{94}H_{131}O_{14}N_{13}$, $C_{97}H_{136}O_{15}N_{14}$, $C_{100}H_{141}O_{16}N_{15}$, and $C_{103}H_{146}O_{17}N_{16}$ (n = 0, 1, 2, 3, and 4, respectively; see Chart 1), 1594, 1667, 1738, 1809, and 1880; found, 1596, 1670, 1739, 1812, and 1884, respectively.

Methods. All fluorescence experiments were carried out in quartz cells, using solutions previously bubbled for about 20 min with ultrapure nitrogen. Steady-state fluorescence spectra were recorded on a SPEX Fluoromax spectrofluorometer, operating in SPC mode, and fluorescence anisotropy measurements were carried out on the same apparatus, equipped with Glan-Thomson polarizing prisms. Nanosecond decays were measured by a homemade SPC apparatus [ORTEC electronics, optics from Applied Photophysics, nanosecond coaxial flashlamp (FWHM = 2.0 ns) from Edinburgh Instruments]. Excitation in the UV region was achieved by ultrapure deuterium as filling gas (0.400 mmHg). The decay curves were fitted by a nonlinear least-squares analysis to exponential functions by an iterative deconvolution method.

Transient absorption measurements were carried out by a flash-photolysis setup, the pulsed excitation (308 nm) being achieved by a Xe/HCl excimer laser (Lamda Physik EMG 50E). The pulse width was about 15 ns, the laser energy < 10 mJ/pulse, and the delay time <1 ns. The light (150 W Xe lamp) was examined through a Baird-Tatlock monochromator and a Hamamatsu R928 photomultiplier and then captured by a Tektronix DSA602 transient digitizer.

Absorption spectra were recorded on a Jasco 7850 apparatus, and circular dichroism (CD) measurements were carried out on a Jasco J-600 instrument with appropriate quartz cells. Molar ellipticities are given on a per residue basis, [Θ′] (deg cm^2 dmol^{-1}), i.e., [Θ′] = (Θ/$n'Cl$), where Θ is the ellipticity (mdeg), C is the peptide concentration (mM), n' is the number of amino acids in the peptide, and l is the optical path length (cm). IR spectra were carried out on a Perkin-Elmer 983 IR spectrophotometer, using CaF_2 cells.

^{1}H NMR spectra were recorded on a Bruker AM 400 instrument operating at 400.135 MHz. The spectral width used was 14 ppm, and a residual water resonance at 4.77 ppm was assumed for chemical shift calibration. Other apparatuses were already reported.[8]

Results and Discussion

Polarized Fluoresence and Differential Circular Dichroism Spectra. Although the chromophores are bound to the main chain by a rather long spacer, i.e., -$(CH_2)_4$-NH-CO-CH_2-naphthalene or -$(CH_2)_4$-NH-CO-$(CH_2)_2$-porphyrin ring, they experience a rotational mobility definitely more hindered than that of peptide-free molecules, primarily ascribable to the presence of the amide bond in the substituted side chains.[1b]

Polarized fluorescence measurements show that the anisotropy coefficient increases on going from the blanks to the peptide solutions and from methanol to the mixed (H_2O–methanol) solvent medium (Table 1). Therefore, the conformational mobility of the probe linkages decreases in the same direction, the enhanced effect in the presence of water being suggestive of intramolecular interactions between the apolar N and P groups, as already observed with the aqueous solution of poly(L-lysine) carrying the same chromophores.[1b]

The DCD spectra in methanol or H_2O–methanol (75/25, v/v) solution are consistent with the aforementioned data. They exhibit extrinsic bands in the ^1B_b and ^1C_b absorption region (220–190 nm) of naphthalene,[1b,2c,13] despite its location far away from the chiral C^α atom (Figure 1). This strongly suggests a hindered conformational mobility of the side chains carrying N,[1b,2a] which is enhanced by the presence of P. Unfortunately, the rotational strength of the peptide groups in the same spectral region prevents a quantitative evaluation of the effect.

Table 1. Fluorescence Anisotropy Coefficients, r,[a] of Oligopeptides in Methanol or H_2O–Methanol (75/25, v/v)

	$10^3 r$	
sample	meth	H_2O–meth
$(Ala)_2N$	0.7	0.9
$P(Ala)_0N$	3.1	15.6
$P(Ala)_1N$	3.1	10.9
$P(Ala)_2N$	6.9	23.0
$P(Ala)_3N$	4.1	n.d.
$P(Ala)_4N$	4.7	50.8

[a] $r = [(I_\parallel - I_\perp)/(I_\parallel + 2I_\perp)]$; λ_{ex} = 280 nm, λ_{em} = 337 nm; reproducibility better than 20%.

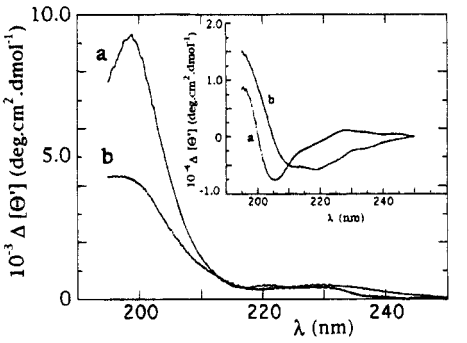

Figure 1. Differential CD spectra of $(Ala)_2N$ vs $(Ala)_2$ in (a) methanol and (b) H_2O–methanol, 75/25 (v/v). Insert: DCD spectra of $P(Ala)_2N$ vs $(Ala)_2$ in the same solvents. The molar ellipticity is on a per residue basis.

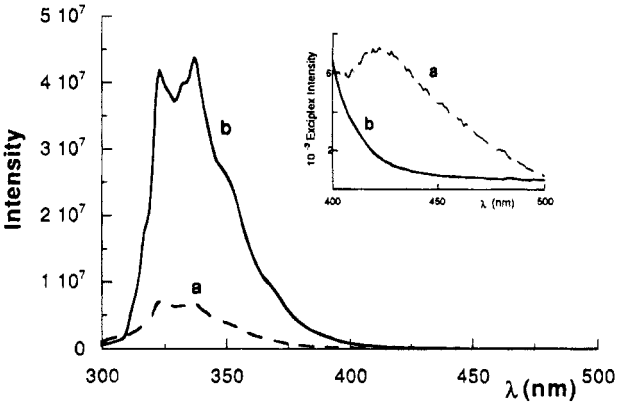

Figure 2. Fluorescence spectrum of the nonapeptide, $P(Ala)_3N$ (a), and of the corresponding blank sample, $(Ala)_3N$ (b), in methanol solution; λ_{ex} = 285 nm. The insert shows the exciplex emission.

Steady-State Fluorescence and Transient Absorption Spectra. Steady-state fluorescence spectra show that exciplex emission (≈425 nm) is definitely minor, a finding that supports the foregoing conclusions.[2b] This is illustrated in Figure 2, where the emission spectra of $P(Ala)_3N$ and $(Ala)_3N$ in methanol solution are reported. Besides the weak exciplex emission (insert in the figure), a substantial quenching of N singlet emission by the bound protoporphyrin molecule can be noted.

The fluorescence quantum yield of the oligopeptides in methanol solution (Φ_{PN}) and the efficiency of the quenching process, E_N, as given by [1 − (Φ_{PN}/Φ_N)], are reported in Table 2. The quantum yield of the blank samples, carrying the N group only (Φ_N), is quite similar to that of free naphthalene,[14] which indicates that

Table 2. Energy Transfer Efficiencies from Steady-State Fluorescence Measurements

sample	Φ_{PN}	E_N[a]	E_P[b]
$P(Ala)_0N$	0.09	0.61	0.58
$P(Ala)_1N$	0.09	0.59	0.53
$P(Ala)_2N$	0.04	0.82	0.78
$P(Ala)_3N$	0.05	0.77	0.66
$P(Ala)_4N$	0.10	0.55	0.43

[a] $E_N = 1 - (\Phi_{PN}/\Phi_N)$, where Φ_{PN} = quantum yield of N* in the samples and $\Phi_N \approx 0.22$ (blanks). [b] $E_P = [(I_{PN}/I_P) - 1](\epsilon_P C_P/\epsilon_N C_N)$, where I_{PN} and I_P are the fluorescence intensities of porphyrin (λ_{ex} = 280 nm, λ_{em} = 630 nm) in the samples and the blanks [$(Ala)_0P$, $(Ala)_1P$, $(Ala)_2P$, etc.], respectively, and C_P and C_N are the concentration of acceptor and donor chromophores, respectively ($I_P = \epsilon_P C_P \Phi_P$; $I_{PN} = \epsilon_P C_P \Phi_P + \epsilon_N C_N \Phi_P E_P$).

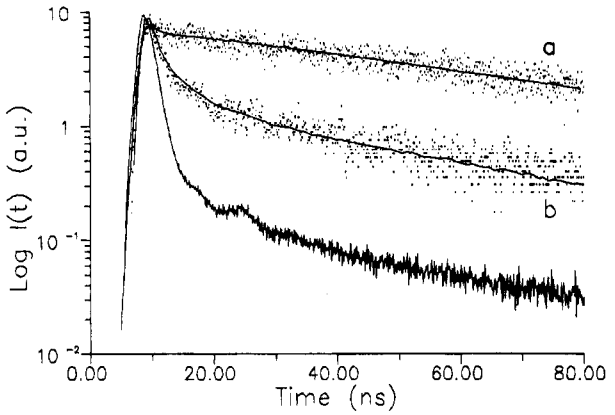

Figure 3. Fluorescence decay profiles (λ_{ex} = 285 nm, λ_{em} = 340 nm) of $(Ala)_3N$ (a) and $P(Ala)_3N$ (b) in methanol. The full lines represent the best fit of the data by a monoexponential decay for the blank and a two-exponential decay for the nonapeptide carrying both N and P. The lamp profile is also shown.

naphthyl–peptide interactions are absent or very weak. By inspection of the table, it appears that the quenching efficiency goes through a maximum as n increases. This suggests that the interchromophoric distance is controlled by factors other than simply the number of alanyl units in the backbone chain. In other words, if chain folding occurs, more Ala intervening residues do not necessarily mean a greater separation distance between the chromophores.

Where the excitation spectra of blank (carrying the P group only) and oligopeptide samples, over the spectral region of N absorption (220–320 nm), are compared, it appears that N contributes to the fluorescence of P, the quantum yield of protoporphyrin in the oligopeptides being definitely larger than that of the corresponding blank samples (Table 2). Since no significant changes were observed by varying sample concentration by 1 order of magnitude, this finding is a strong indication that intramolecular N* → P energy transfer takes place.

We next investigated the transient absorption spectra of both blank and oligopeptide samples in methanol solution. A typical example is shown in Figure 3, where the characteristic triplet–triplet absorption of protoporphyrin at λ_{max} = 320 and 470 nm[15,16] and the weak absorption structures at lower energies, possibly ascribable to radical anions, are observed. These spectra exhibit quite similar features for all the compounds examined. The lifetimes of the triplet states were found to be of the order of 11–13 μs, while kinetic measurements of oxygen saturation following laser excitation show that the second-order rate constant for bleaching the 320 and 470 nm absorptions is around 1.8×10^9 M^{-1} s^{-1}. This figure closely agrees with the second-order rate constants for triplet quenching by O_2.[15-17]

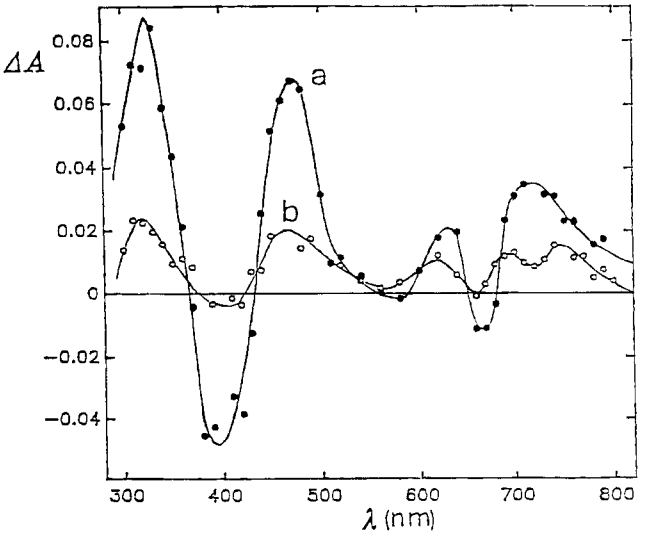

Figure 4. Transient absorption spectra of $P(Ala)_3N$ in methanol, after 1.1 μs (a) and 21.2 μs (b).

Both the observation that no absorption in the transient spectra can be ascribed to a radical cationic moiety[1,17] and the foregoing results on the emission behavior of porphyrin (Table 2) lead us to conclude that quenching of naphthalene by porphyrin can not be due to a P → N* electron transfer process, as previously observed with α-helical poly(L-lysine) carrying the same chromophores,[1,18] but rather to the electronic energy transfer between the energetically excited donor (N*) and the ground-state acceptor (P).

Fluorescence Time Decay. Typical decay profiles in methanol solution of excited naphthalene (λ_{ex} = 280 nm, λ_{em} = 340 nm) are shown in Figure 3. No significant change was observed on varying sample concentration within 1 order of magnitude (5×10^{-6}–5×10^{-5} M), which rules out the occurrence of interchain effects.

$$\langle\tau\rangle = \alpha_1\tau_1 + \alpha_2\tau_2 \quad (1)$$

$$E' = 1 - (\langle\tau\rangle/\tau_0) \quad (2)$$

The curves are well described by a two-component exponential decay, the average decay time, $\langle\tau\rangle$, being given by eq 1 and the overall quenching efficiency, E', by eq 2, where τ_0 is the time decay of the blank samples, always found to be strictly monoexponential. Therefore, the overall transfer efficiency must be read as $E' = \alpha_1 E_1 + \alpha_2 E_2$, where E_i (i = 1 and 2) is given by eq 3.

$$E_i = 1 - (\tau_i/\tau_0) \quad (3)$$

In all cases, comparison between the overall quenching efficiencies of steady-state, $1 - (\Phi_{PN}/\Phi_N)$, and time-resolved, $1 - (\langle\tau\rangle/\tau_0)$, fluorescence is good, within experimental errors. This suggests that a fast quenching process or (strong) ground-state interactions are absent.

Of the two lifetime components, the shorter one (τ_1 = 3–8 ns) is predominant and varies with the number of alanyl units in the main chain, suggesting that it is related to the energy transfer process. The longer lifetime ($\tau_2 \approx 45$ ns) is, instead, insensitive to peptide composition and was thus assigned to the decay of exciplexes. However, the preexponent of the long component varies with the length of the peptides, being much larger for the hepta- and decapeptide than for the

Table 3. Time Decay Parameters of Intramolecular Energy Transfer in the Sequential Peptides[a]

sample	τ_1 (ns)	α_1	τ_2 (ns)	α_2	χ^2
$P(Ala)_0N$	8.3	0.85	45.5	0.15	1.40
$P(Ala)_1N$	4.1	0.62	46.0	0.38	1.15
$P(Ala)_2N$	3.1	0.93	45.6	0.07	1.05
$P(Ala)_3N$	7.1	0.82	44.2	0.18	1.18
$P(Ala)_4N$	6.5	0.59	46.0	0.41	1.53

[a] In methanol, at 25 °C. The time decay of the blank samples is $\tau_0 = 52.5 \pm 1.5$ ns. The lifetime uncertainty is less than 5%.

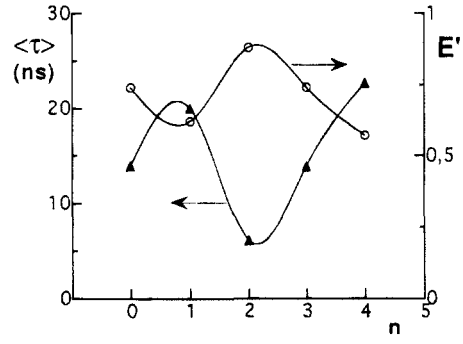

Figure 5. Dependence of the average decay time of excited naphthalene, $\langle\tau\rangle$ (eq 1), and of the overall quenching efficiencies from lifetime measurements, E' (eq 2), on the number of alanyl units, n, in the oligopeptides investigated.

other samples (Table 3). This is very likely because the probes in $P(Ala)_1N$ and $P(Ala)_4N$ are on the same side of the α-helix, one or two turns apart, respectively, thus favoring exciplex formation.

Table 3 lists the values of τ_1 and τ_2, while Figure 5 illustrates the trend of both $\langle\tau\rangle$ and E' as a function of n. Since the number of alanines would be synonymous with a fixed distance of 3.8 Å/residue (shortest through-space distance) or 4.4 Å/residue (through-bond distance) in a fully stretched framework, the peculiar change of both the average relaxation time and the overall efficiency of naphthalene quenching with the number of alanine residues strongly suggests that folded structures form in methanol, so as to vary the interchromophoric distance as compared to that based on the number of alanyl units alone.

IR and CD Spectra. Short linear peptides, in which both amino and carboxyl terminii are derivatized, are in general considered to be unordered in protic media because competition for intermolecular H-bond interactions by solvent tends to diminish the advantage of folded structure stabilization by intramolecular H-bonds. Nevertheless, a number of studies have recently shown that this kind of peptide is able to attain ordered conformations in solution,[19-24] as also suggested by the foregoing results on the short Leu- and Ala-based peptides (Chart 1). We then investigated the conformational features of these compounds by IR and CD spectra, while ^1H NMR measurements are under way.

The most informative IR frequency ranges for the peptides are the following: (1) 3540–3270 cm^{-1}, corresponding to the N–H stretching vibrations of peptide (amide A region) and urethane groups, and (2) 1800–1600 cm^{-1}, corresponding to the C=O stretching vibrations of peptide (amide I region), urethane, and ester groups.

Blank samples (carrying P or N group only) in CD_3OD solution at concentrations around 1×10^{-4}–3×10^{-4} M exhibit a band of low intensity in the frequency range of 3330–3320 cm^{-1} and a definitely more intense band in the 3425–3435 cm^{-1} region. The former

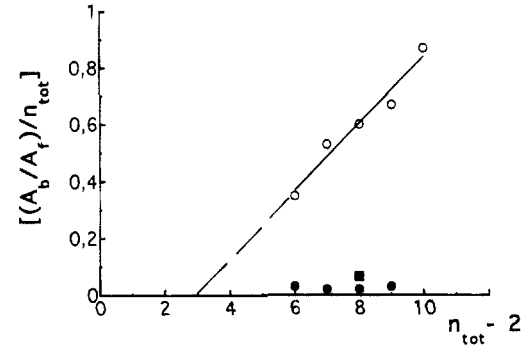

Figure 6. Plot of $(A_b/A_f)/n_{tot}$ against $n_{tot} - 2$ for $P(Ala)_nN$ (empty symbols) and blank samples (full symbols; circles, $(Ala)_nN$; squares, $(Ala)_nP$). n_{tot} denotes the number of amide groups in the peptides, including those in the side chains (see text). The ratio $(A_b/A_f)/n_{tot}$ represents an empirical index of the restructuring effects of bound N and P molecules on the peptides.

absorption refers to H-bonded N–H groups, while the latter is indicative of the occurrence of free (or extremely weakly H-bonded) N–H groups.[23,25] Since the intensities of these bands vary linearly as the concentration increases by 1 order of magnitude, one may safely conclude that absorption at around 3330 cm^{-1} refers to intramolecular H-bonded N–H groups. According to the integrated intensity of these bands, the H-bonded N–H groups in blank samples are less than 10%, but they dramatically increase in the oligopeptides carrying both chromophores, a finding suggestive of concerted restructuring effects of the bound N and P groups. This is confirmed by the spectral results in the amide I region, where all peptides exhibit a major absorption at around 1650–1660 cm^{-1}, typical of C=O stretching of H-bonded peptide moieties.[25] Instead, the C=O stretching of free peptide groups is normally observed in the 1670–1700 cm^{-1} region, as found by us in the blank samples (~1672 cm^{-1}), while the C=O stretching of the *tert*-butyl ester (OtBu) is found at 1725–1730 cm^{-1}.

Where A_b and A_f are the integrated intensities of the bands of H-bonded and free N–H groups at around 3325 and 3430 cm^{-1}, respectively, the $(A_b/A_f)/n_{tot}$ ratio represents an empirical index of the restructuring effects of N and P moieties on the compounds examined, n_{tot} being the total number of amide groups, including both the urethane group in the backbone[26] and the two NH–CO groups in the probe linkages. By plotting this quantity against $n_{tot} - 2$, a straight line is obtained, as shown in Figure 6. The intercept at $(A_b/A_f)/n_{tot} = 0$, which corresponds to the number of peptide groups in the backbone chain that are one unit too short for a helical turn formation by an intramolecular hydrogen bond, is $n_{tot} - 2 = 3$. This result is surprisingly good since this figure is that expected for an α-helical structure whose H-bonding scheme is of the $i \rightarrow i + 4$ (C_{13}) type.

Two other points are worth noting. First, in all cases the urethane moiety (Boc) very likely acts as a "peptide" group so as to contribute to the folding process in the compounds examined.[26] This is particularly true for the hexapeptide, $P(Ala)_0N$, that otherwise would not even exhibit the lowest tendency to attain a helical conformation. Second, the samples carrying the N or P group only (blanks) have an A_b/A_f ratio nearly zero, thus confirming the idea that both probes do exert a concerted restructuring effect on the peptides.

We next examined the CD spectra in methanol and water–methanol solutions, reported in Figures 7 and

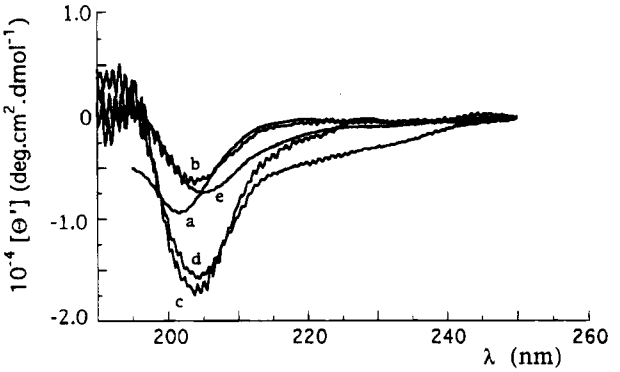

Figure 7. Circular dichroism spectra of P(Ala)$_n$N in methanol solution, from $n = 0$ (curve a) to $n = 4$ (curve e). Concentration is 2.5×10^{-4}–5.0×10^{-4} M in all cases.

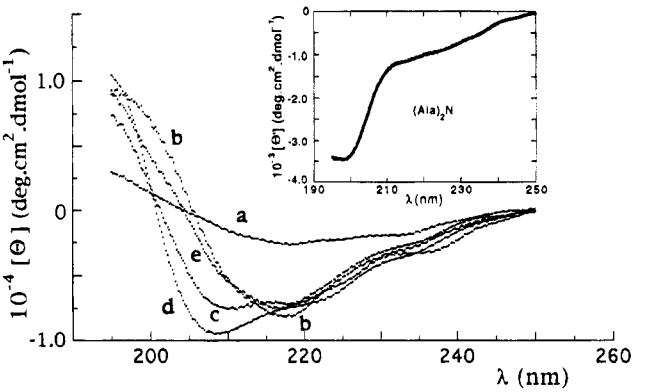

Figure 8. CD spectra as those of Figure 7 but in water–methanol, 75/25 (v/v). Insert: CD spectrum of (Ala)$_2$N in the same mixture.

8, respectively. In agreement with the foregoing conclusion, these patterns suggest that even the shortest member of the series populates ordered structures, otherwise the lower energy band would have been centered below 200 nm.[21] This is indeed the case for the triad, whose spectrum is characteristic of random coil, with the lowest energy band in the spectrum being centered at around 198 nm ([Θ'] = −6620 deg cm^2 dmol^{-1} in methanol).[8,21a] In addition, the red shift of this band on going from P(Ala)$_0$N to P(Ala)$_4$N is indicative of increasing amounts of ordered conformations. Interestingly, in the absence of self-association, the IR frequencies of the absorption maxima of the stretching modes of intramolecularly H-bonded N—H and C=O groups (see above) parallel with these changes in that they decrease from 3330 to 3322 cm^{-1} and from 1663 to 1658 cm^{-1}, respectively, as the peptide chain length increases.

The population of ordered conformations in methanol solution that is deducible from the ellipticity at 222 nm[7,19] seems, however, smaller than that suggested by IR data. This apparent discrepancy may be reconciled by taking into account the theoretical results reported by Woody et al. on CD spectra of distorded α-helices.[27] Systematic distortions due to the dynamic fluctuation of the α-helical conformation bring about significant changes in the spectrum of short linear peptides. For instance, the rotational strength in the $n\pi^*$ absorption region decreases upon tilting of C=O groups.[27] This may be the reason why the oligopeptides investigated have a weak rotational strength at around 220 nm despite the fact that organic solvents, such as alcohols, stabilize the α-helical conformation in linear peptides and polypeptides.[28,29]

When water is added to the methanol solution, the CD patterns change dramatically, as illustrated in Figure 8, the shape of the curves now closely resembling that of α-helix.[7,19,30] This finding can be interpreted as due to hydrophobic interactions between the apolar N and P groups that slow down the dynamic distortions of the ordered structure occurring in methanol solution,[27] thus stabilizing the α-helical conformation. The data of both fluorescence anisotropy and differential CD measurements in the mixed solvent (Table 1, Figure 1), as well as the CD spectra of the blanks (insert of Figure 8), support this conclusion. To summarize, the results of IR and CD spectra suggest that the Leu- and Ala-based peptides investigated are likely to attain an α-helical structure in solution, but variable amounts of random coil are also present, depending on the chain length.[23b]

Conformational Statistics. Owing to both the position of the C$^\alpha$ atom of the probe linkages in the ordered backbone chain, which varies as the number of Ala residues increases, and the conformational mobility of the aliphatic portion of these linkages, one can expect a distribution of interchromophoric separation distances. In addition, the results of polarized fluorescence and DCD measurements suggest that the internal rotation of the chromophores is probably slow on the time scale of the transfer process because the amide bond in the substituted side chains hinders the rotational Brownian motion.[1b] We then evaluated the probability distribution of center-to-center distances of chain-linked donor–acceptor pairs by means of a conformational statistics analysis on the α-helical peptides, since spectral results indicate that this structure predominates in solution. For the purpose, a rotational isomeric states model was employed, in which rotation around each of the seven or eight single bonds of the lysine side chains, depending on the bound chromophore, is restricted to a few highly populated, low-energy isomeric states.[10,11] By discarding the conformations g^+g^- and g^-g^+ for the aliphatic portion of these chains, owing to their very low probability, and those conformations in which the chromophore is less than 5 Å from the helical axis, for steric reasons, the number of conformers are 1836 for P linkage and 609 for N linkage, the actual distribution of conformations being thus assumed to be well represented with these restrictions.

Table 4 lists the rotational isomeric states, relative energies, and statistical weights for the donor and acceptor linkages in the peptides, while the geometrical parameters used for the calculations are illustrated in Figure 9, where each bond in the acceptor chromophore linkage is denoted as j and numbered from 1 to 9 while that in the donor chromophore linkage is k and numbered from 10 to 17.

If one assumes the simplest model, i.e., that in which the population distribution among the states of each bond is independent of the other bonds in the linkage, the conformational partition function can be factored into a product of individual partition functions, one from each bond, i.e.,

$$Q' = \prod_{j=1}^{9} q_j \prod_{k=10}^{17} q_k \qquad (4)$$

where the products are formed from all the bonds of the linkages, and

Table 4. Relative Energies and Statistical Weights of the Rotational Isomeric States of the Donor (N*) and Acceptor (P) Linkages[a]

bond rotational angle[b]		rotat isomeric state[c]	energy, $E_{jl(kl)}$[d]	$w'_{j(k)}$[e]	$q_{j(k)}$[f]
χ_1	χ_{10}	+60	0	1	
		−60	0	1	3
		180	0	1	
χ_2	χ_{11}	+60	0.5	exp(−0.5/*RT*)	
		−60	0.5	exp(−0.5/*RT*)	1 + 2 exp(0.5/*RT*)
		180	0	1	
χ_3	χ_{12}	+60	0.5	exp(−0.5/*RT*)	
		−60	0.5	exp(−0.5/*RT*)	1 + 2 exp(−0.5/*RT*)
		180	0	1	
χ_4	χ_{13}	+60	0.5	exp(−0.5/*RT*)	
		−60	0.5	exp(−0.5/*RT*)	1 + 2 exp(−0.5/*RT*)
		180	0	1	
χ_5	χ_{14}	+60	0	1	
		−60	0	1	3
		180	0	1	
χ_6	χ_{15}	180	0	1	1
χ_7	χ_{16}	+60	0	1	
		−60	0	1	3
		180	0	1	
χ_8	−	+60	0.5	exp(−0.5/*RT*)	
		−60	0.5	exp(−0.5/*RT*)	1 + 2 exp(−0.5/*RT*)
		180	0	1	
χ_9	χ_{17}	+90	0	1	
		−90	0	1	2

[a] The values of both relative energies, $E_{jl(kl)}$, and statistical weights of the rotational isomeric states are based on conformational analysis data of compounds containing similar structural elements.[11] [b] Dihedral angles, as illustrated in Figure 9. The rotational angles referring to the acceptor chromophore linkage (χ_j) are listed in the first column, and those referring to the donor chromophore linkage (χ_K) are in the second column. [c] The definition of the angles conforms to IUB-IUPAC recomandations. [d] In kcal/mol. [e] The statistical weight is given by $\exp(-E_{jl(kl)}/RT)$. [f] The bond partition function is given by $q_{j(k)} = \sum_l \exp(-E_{jl(kl)}/RT)$, where the sum is taken over all states l of bond j or k, respectively.

$$q_{j(k)} = \sum_l \exp(-E_{jl(kl)}/RT) \tag{5}$$

is the partition function of the jth (kth) bond, where $E_{jl(kl)}$ is the relative energy of bond $j(k)$ when in state l, and the sum is taken over all states l of bond $j(k)$. From the data of Table 4, one has $Q' = 2916[1 + 2\exp(-0.5/RT)]^7 = 2.25 \times 10^5$ (298 K). However, by discarding both the v conformations in which the chromophores are closer than 5 Å to the helical axis and the g^+g^- and g^-g^+ conformations, the partition function can be written as eq 6

$$Q = Q' - (\prod_j q_j \prod_k q_k)_{g^\pm g^\mp, v} \tag{6}$$

where $Q = 8.30 \times 10^4$ (298 K).

The average transfer efficiency, $\langle E \rangle$, can be now calculated by eq 7, where w_m and E_m are the statistical weight and the transfer efficiency for each conformation m, as given by eqs 8 and 9, respectively, and the sum is taken overall conformation of both donor and acceptor chromophore linkages.

$$\langle E \rangle = \frac{\sum_m w_m E_m}{Q} \tag{7}$$

$$w_m = \prod_{j=1}^{9} w'_j \prod_{k=10}^{17} w'_k \tag{8}$$

The products in eq 8 are taken over all bonds j and k of the acceptor and donor chromophore linkages, respectively, and w'_j and w'_k are the statistical weights assigned to bond j when in state l' and to bond k when in state l, respectively. On the other hand, R_m in eq 9 is the center-to-center distance when the peptide side chains populate the conformation m, and k^2_m is a dimensionless geometric factor determined by the orientation in space of the transition dipole moments of the donor and acceptor, as given by eq 10.[31]

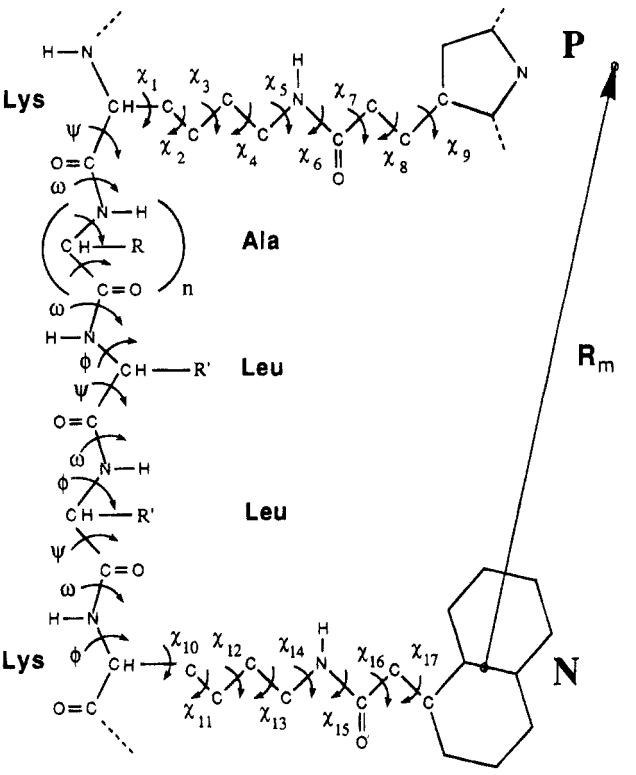

Figure 9. Notation and structural geometry of the peptides investigated, showing the rotational angles of the P and N chromophore linkages (χ) and those of the main chain fixed at $\phi = -57°$, $\psi = -47°$, $\omega = 180°$ (α-helix). The intramolecular center-to-center distance for a given conformation, m, of the chromophore linkages is denoted as $R_m = |\mathbf{R}_m|$. Hydrogen atoms are omitted for clarity, while the side chains are R = CH_3 and R′ = $CH_2CH(CH_3)_2$.

Chart 2

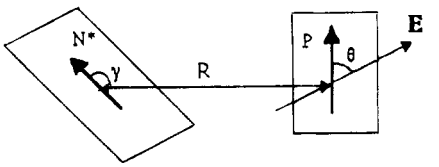

$$E_m = [1 + [2/(3k^2_m)](R_m/R_0)^6]^{-1} \tag{9}$$

$$k^2_m = \cos^2\theta(3\cos^2\gamma + 1) \tag{10}$$

Provided that the donor and acceptor molecules do not rotate fast enough to randomize their orientation during the donor lifetime, a particular relative orientation between the probes is described by two angles only, γ and θ, where $0 \le \gamma$ and $\theta \le \pi$. The scheme used to evaluate the orientations in space of the transition dipole moments of N* and P is illustrated in Chart 2.[32] Instead, when random relative orientations occur, the "dynamic" isotropic average of the orientation factor, $\langle k^2 \rangle = {}^2/_3$, is used.[2b,11,12,33,34]

Correlation between Energy Transfer and Structural Features of the Peptides. Two conditions must

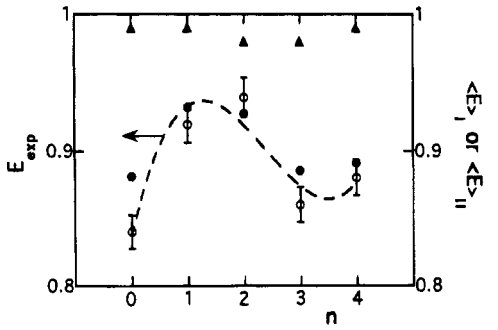

Figure 10. Energy transfer efficiencies $\langle E\rangle_I$, calculated according to eq 7 with k^2 given by eq 10 for each conformation m (k^2_m) and the geometry illustrated in Chart 2 for the transition dipole moments (●), or $\langle E\rangle_{II}$, calculated according to eq 7 with $k^2_m = \langle k^2\rangle = {}^2/_3$ (▲). The experimental transfer efficiencies from lifetime results, E_{exp} (eq 3), are also reported for comparison (○).

be matched for energy transfer to occur. The first is a spectral requirement, i.e., the emission spectrum of the donor must overlap with the absorption spectrum of the acceptor. The second is a geometric requirement, i.e., the emission and absorption dipoles of the donor and acceptor molecules, respectively, must be at a certain distance and properly oriented.

The first requirement is related to the apparent transfer radius, R_0, which was evaluated by eq 11,[9,31] where n is the refractive index, N_0 is Avogadro's number, Φ_N is the donor fluorescence quantum yield in the absence of transfer, $\epsilon_A(\lambda)$ (M^{-1} cm^{-1}) is the extinction coefficient of the acceptor, and J is given by eq 12, where the integral of the donor fluorescence is normalized to unity.

$$R_0^6 = \{[^2/_3(\ln 10)\, 9.10^3\, \Phi_N]/[128\, \pi^5\, n^4\, N_0]\}\cdot J \quad (11)$$

$$J = \frac{\int_0^\infty F_D(\lambda)\epsilon_A(\lambda)\lambda^4\, d\lambda}{\int_0^\infty F_D(\lambda) d\lambda} \quad (12)$$

From the results, the spectral overlap integral is 1.30×10^{-13} M^{-1} cm^3, and hence $R_0 = 42.2$ Å.

To evaluate the interchromophoric distance, R, by transfer efficiency when distance distribution is ignored, eq 13 is commonly used, the transfer efficiency being measured by fluorescence intensity and/or fluorescence lifetimes.[35]

$$E = R_0^6/(R_0^6 + R^6) \quad (13)$$

By using this equation, the values of R are seen to vary, e.g., from about 32 Å for the hexapeptide to 27 Å for the octapeptide. Since these figures are too large to account for the actual interchromophoric separation distance, not unexpectedly it appears that the probability distribution of center-to-center distances between the probes can not be ignored. We then calculated the transfer efficiencies by eqs 7–9. In principle, two transfer efficiencies can be evaluated, one based on the assumption that the rotational Brownian motion is frozen as compared to the time scale of the transfer process, which implies the use of eq 10, and the other based on the assumption of free internal rotation, i.e., $k^2_m = \langle k^2\rangle = {}^2/_3$. These transfer efficiencies, here denoted as $\langle E\rangle_I$ and $\langle E\rangle_{II}$, respectively, are reported in Figure 10 together with that experimentally determined

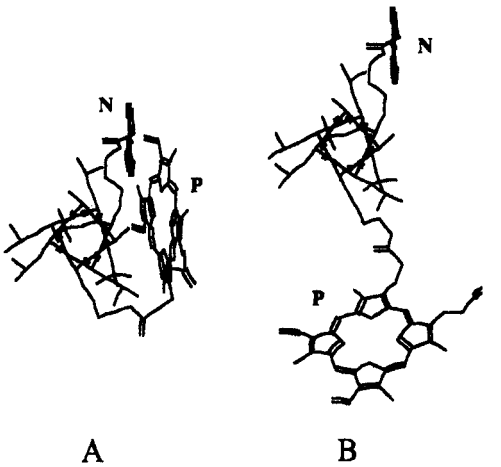

Figure 11. Molecular structures of two allowed conformations of $P(Ala)_2N$, viewed along the helical axis. The center-to-center distance between the P and N chromophores is about 7 Å (A) and 21 Å (B); see text.

by lifetime results, i.e., $E_{exp} = 1 - (\tau_1/\tau_0)$ (eq 3), since only the short time decay component varies with n. As may be seen, only the values of $\langle E\rangle_I$ compare satisfactorily with E_{exp}, confirming the idea that biased chromophore orientations contribute to the measured distances.

Finally, if transfer efficiency would depend on the α-helix periodicity only, $P(Ala)_2N$ should experience the lowest efficiency because its probe linkages are farther away than in the other peptides. This is not the case, however, because both the length and flexibility of the aliphatic portion of the chromophore linkages are such as to bring the probes near each other, even when the C^α atoms of these linkages are five residues apart, as in $P(Ala)_2N$. This is exemplified in Figure 11, where two allowed conformations of the octapeptide are presented. In one case (Figure 11A) the N and P chromophores are close to each other, while in the other one (Figure 11B) they are separated by a relatively large distance. If the former structure was a low-energy conformation, it would heavily contribute to the transfer process. On the other hand, the efficiency of the process also depends on the mutual orientations of the probes. As a result, the trend of Figure 10 is obtained.

Although the model employed to estimate the interprobe distance distributions does not take into account complicated phenomena, such as, e.g., interactions between neighboring bonds or self-intersection, that might affect the values of R_m and hence E_m, the agreement between experimental and calculated transfer efficiencies is good, provided that the orientations in space of the transition dipole moments of the donor and acceptor were properly considered.

Concluding Remarks

The short linear Leu- and Ala-based peptides investigated attain an α-helical conformation in methanol solution, which is stabilized by increasing the length of the backbone chain. The ordered structure is also stabilized by adding water that favors intramolecular hydrophobic interactions between the apolar N and P groups. The relative position of the chromophores in the peptides depends on both the α-helical periodicity of the C^α atoms of the lysine side chains carrying the chromophores, which varies with increasing the Ala residues in the backbone, and the conformational mobility of the aliphatic portion of these chains. The probability distribution of the interprobe distances was

successfully evaluated by a rotational isomeric states model, but orientational effects between the P and N groups had to be also taken into account for a correct interpretation of fluorescence decay data because interconversion among conformational substates of probe linkages is slow on the time scale of the transfer process.

Acknowledgment. We wish to thank Prof. N. Rosato and Dr. F. Elisei for helpful discussions and Mr. G. D'Arcangelo for technical assistance. This work was supported in part by MURST (Rome) and in part by the National Research Council (CNR).

References and Notes

(1) (a) Pispisa, B.; Venanzi, M.; D'Alagni, M. *Biopolymers* **1994**, *34*, 435–442. (b) Pispisa, B.; Venanzi, M.; Palleschi, A. *J. Chem. Soc., Faraday Trans.* **1994**, *90*, 1857–1864.

(2) (a) Sisido, M.; Tanaka, R.; Inai, Y.; Imanishi, Y. *J. Am. Chem. Soc.* **1989**, *111*, 6790–6796. Inai, Y.; Sisido, M.; Imanishi, Y. *Ibid.* **1991**, *95*, 3847–3851. (b) Inai, Y.; Sisido, M.; Imanishi, Y. *J. Phys. Chem.* **1990**, *94*, 6237–6243, 8365–8370. (c) Sisdo, M.; Egusa, S.; Imanishi, Y. *J. Am. Chem. Soc.* **1983**, *105*, 1041–1049.

(3) (a) Isied, S. S. In *Metal Ions in Biological Systems*; Siegel, H., Sigel, A., Eds.; Dekker: New York, 1991; Vol. 27, pp 1–56. (b) Isied, S. S.; Ogawa, M. Y.; Wishart, J. F. *Chem. Rev.* **1992**, *92*, 381–394 and references cited therein.

(4) Schanze, K. S.; Sauer, K. *J. Am. Chem. Soc.* **1988**, *110*, 1180–1186. Schanze, K. S.; Cabana, L. A. *J. Phys. Chem.* **1990**, *94*, 2740–2743.

(5) Stryer, L.; Haugland, R. P. *Proc. Natl. Acad. Sci. U.S.A.* **1967**, *58*, 719–726.

(6) Chou, P. Y.; Fasman, G. D. *Annu. Rev. Biochem.* **1978**, *47*, 251–276.

(7) Marqusee, S.; Robbins, V. H.; Baldwin, R. L. *Proc. Natl. Acad. Sci. U.S.A.* **1989**, *86*, 5286–5290.

(8) Pispisa, B.; Venanzi, M.; Palleschi, A.; Zanotti, G. *J. Mol. Liq.* **1994**, *61*, 167–187.

(9) Förster, T. *Ann. Phys. (Leipzig)* **1948**, *2*, 55–75.

(10) Flory, P. J. *Statistical Mechanics of Chain Molecules*; Interscience: New York, 1969.

(11) McWherter, C. A.; Haas, E.; Leed, A. R.; Scheraga, H. A. *Biochemistry* **1986**, *25*, 1951–1963.

(12) Valeur, B.; Mugnier, J.; Pouget, J.; Bourson, J.; Santi, F. *J. Phys. Chem.* **1989**, *93*, 6073–6079. Kaschke, M.; Ernsting, N. P.; Valeur, B.; Bourson, J. *Ibid.* **1990**, *94*, 5757–5761.

(13) Jaffé, H. H.; Orchin, M. *Theory and Applications of Ultraviolet Spectroscopy*; Wiley: New York, 1962; Chapter 13.

(14) Eaton, D. F. *Pure Appl. Chem.* **1988**, *60*, 1107–1114.

(15) Sinclair, R. S.; Tait, D.; Truscott, T. G. *J. Chem. Soc., Faraday Trans. 1* **1980**, *76*, 417–425.

(16) Chatterjee, P. K.; Kamioka, K.; Batteas, J. D.; Webber, S. E. *J. Phys. Chem.* **1991**, *95*, 960–965.

(17) Nahor, G. S.; Rabani, J.; Grieser, F. *J. Phys. Chem.* **1981**, *85*, 697–702.

(18) Pispisa, B.; Palleschi, A.; Venanzi, M. *Trends Phys. Chem.* **1991**, *2*, 153–183.

(19) Padmanabhan, S.; Marqusee, S.; Ridgeway, T.; Laue, T. M.; Baldwin, R. L. *Nature (London)* **1990**, *344*, 268–270.

(20) (a) Karle, I. L.; Flippen-Anderson, J. L.; Uma, K.; Balaram, H.; Balaram, P. *Biopolymers* **1990**, *29*, 1433–1442. (b) Parthasarathy, R.; Kuantee, G.; Chaturvedi, S. *Ibid.* **1993**, *33*, 163–171.

(21) (a) Kawai, M.; Fasman, G. *J. Am. Chem. Soc.* **1978**, *100*, 3630–3632. (b) Imperiali, B.; Fisher, S. L.; Moats, R. A.; Prins, T. J. *J. Am. Chem. Soc.* **1992**, *114*, 3182–3188.

(22) (a) Malcolm, B. R. *Biopolymers* **1983**, *22*, 319–322. (b) Basu, G.; Bagchi, K.; Kuki, A. *Ibid.* **1991**, *31*, 1763–1774.

(23) (a) Benedetti, E.; Bavoso, A.; Di Blasio, B.; Pavone, V.; Pedone, C.; Crisma, M.; Bonora, G. M.; Toniolo, C. *J. Am. Chem. Soc.* **1982**, *104*, 2437–2444. Toniolo, C.; Benedetti, E. *Macromolecules* **1991**, *24*, 4004–4009. (b) Benedetti, E.; Di Blasio, B.; Pavone, V.; Pedone, C.; Santini, A.; Crisma, M.; Toniolo, C. In *Molecular Conformation and Biological Interactions*; Balaram, P., Ramaseshan, S., Eds.; Indian Academy of Science: Bangalore, 1991; pp 497–502.

(24) Miick, S. M.; Martinez, G. V.; Fiori, W. R.; Todd, A. P.; Millhauser, G. L. *Nature (London)* **1992**, *350*, 653–655.

(25) (a) Aubry, A.; Protas, J.; Boussard, G.; Marraud, M.; Neél, J. *Biopolymers* **1978**, *17*, 1693–1711. (b) Pulla Rao, Ch.; Nagaraj, R.; Rao, C. N. R.; Balaram, P. *Biochemistry* **1980**, *19*, 425–431.

(26) Benedetti, E.; Pedone, C.; Toniolo, C.; Nemethy, G.; Potthe, M. S.; Scheraga, H. A. *Int. J. Pept. Protein Res.* **1980**, *16*, 156–172.

(27) Manning, M. C.; Illangesekare, M.; Woody, R. W. *Biophys. Chem.* **1988**, *31*, 77–86.

(28) Brack, A.; Spach, G. *J. Am. Chem. Soc.* **1981**, *103*, 6319–6323.

(29) Barteri, M.; Pispisa, B. *Biopolymers* **1973**, *12*, 2309–2327.

(30) Tiffany, M. L.; Krimm, S. *Biopolymers* **1968**, *6*, 1379–1382. Myer, Y. P. *Macromolecules* **1969**, *2*, 624–628.

(31) (a) Steinberg, I. Z. *J. Chem. Phys.* **1968**, *48*, 2411–2413. (b) Grinvald, A.; Haas, E.; Steinberg, I. Z. *Proc. Natl. Acad. Sci. U.S.A.* **1972**, *69*, 2273–2277.

(32) The geometric parameters used to calculate k^2 are defined as follows (Chart 2). R denotes the distance between the center of mass of N* and P, γ is the angle which the transition dipole moment of N* makes with the line joining the center of mass of N* and P, **E** is the vector representing the electric field at the center of mass of P by the transition dipole moment of N*, and θ is the angle between **E** and the transition dipole moment of P. The magnitude of **E** is the vectorial sum of its radial and angular components, i.e., it is proportional to $[(2\cos\gamma)^2 + \sin^2\gamma]^{1/2} = (3\cos^2\gamma + 1)^{1/2}$.[31a] The component of **E** along the transition dipole moment of P, E_P, is thus proportional to $\cos\theta(3\cos^2\gamma + 1)^{1/2}$, and the value of k^2 that gives the E_P^2 dependence on the orientations of both N* and P is then given by eq 10.

(33) Bednár, B.; Morawetz, H.; Shafer, J. A. *Macromolecules* **1985**, *18*, 1940–1944.

(34) Liu, G. *Macromolecules* **1993**, *26*, 1144–1151.

(35) Lakowicz, J. R. *Principles of Fluorescence Spectroscopy*; Plenum Press: New York, 1983; Chapter 10.